

## Photon scattering by a three-level emitter in a one-dimensional waveguide

D Witthaut<sup>1,2,3</sup> and A S Sørensen<sup>1</sup>

<sup>1</sup> QUANTOP, The Niels Bohr Institute, University of Copenhagen, DK-2100 Copenhagen, Denmark

<sup>2</sup> Max-Planck-Institute for Dynamics and Self-Organization, D-37073 Göttingen, Germany

E-mail: [dirk.witthaut@nbi.dk](mailto:dirk.witthaut@nbi.dk)

*New Journal of Physics* **12** (2010) 043052 (18pp)

Received 21 December 2009

Published 30 April 2010

Online at <http://www.njp.org/>

doi:10.1088/1367-2630/12/4/043052

**Abstract.** We discuss the scattering of photons from a three-level emitter in a one-dimensional waveguide, where the transport is governed by the interference of spontaneously emitted and directly transmitted waves. The scattering problem is solved in closed form for different level structures. Several possible applications are discussed: the state of the emitter can be switched deterministically by Raman scattering, thus enabling applications in quantum computing such as a single-photon transistor. An array of emitters gives rise to a photonic band gap structure, which can be tuned by a classical driving laser. A disordered array leads to Anderson localization of photons, where the localization length can again be controlled by an external driving.

<sup>3</sup> Author to whom any correspondence should be addressed.

**Contents**

<b>1. Introduction</b>	<b>2</b>
<b>2. Single photons in nanoscale waveguides</b>	<b>3</b>
<b>3. Scattering by a three-level atom</b>	<b>6</b>
3.1. Electromagnetically induced transparency in a driven $\Lambda$ -system . . . . .	6
3.2. A $\Lambda$ -system with two coupling transitions . . . . .	8
3.3. Driven V-type atom . . . . .	9
3.4. A V-type atom with two coupling transitions . . . . .	10
<b>4. Applications</b>	<b>11</b>
4.1. A single-photon transistor . . . . .	11
4.2. Tunable photonic band gaps . . . . .	13
4.3. Tunable Anderson localization of photons . . . . .	15
<b>5. Conclusion and outlook</b>	<b>16</b>
<b>Acknowledgments</b>	<b>17</b>
<b>References</b>	<b>17</b>

**1. Introduction**

The effects of spontaneous emission have been extensively explored in two limits. In the weak coupling limit, spontaneous emission is essentially viewed as irreversible loss and a source of decoherence. On the contrary, excitations are periodically exchanged between an emitter and the modes of a cavity in the regime of strong coupling. A different regime is explored in one-dimensional waveguides, where photon scattering is governed by the interference of the absorbed, re-emitted, and the directly transmitted wave. For a simple two-level emitter, this leads to a complete reflection if the photon is resonant with the atomic transition [1]–[3]. In the present paper, we discuss photon scattering from a three-level emitter, which can lead to richer structures in the reflection and transmission.

In order to reach the one-dimensional regime, the coupling to the waveguide has to be strong compared to transversal losses. The strong coupling regime has been first realized in a high- $Q$  resonator for optical or microwave photons (see e.g. [4, 5]). Later, strong coupling was also demonstrated in nanoscale integrated devices using photonic crystal microcavities [6, 7]. In such a cavity, however, the emitter couples only to a discrete set of modes and not to a one-dimensional continuum as in a waveguide. Great advances in the effort to reach the regime of strong coupling also in this situation have been reported only recently using several different systems such as photonic crystal waveguides [8], semiconductor or diamond nanowires [9, 10], optical microfibers [11, 12], hollow core fibers [13] or microwave transmission lines [14]. Another opportunity is to exploit the strong localization of surface plasmon polariton (SPP) modes along a metallic nanowire [15]–[18]. Strong coupling seems to be feasible even in free space if the photons are focused appropriately [19]. Some of these different setups are sketched in figure 1. Owing to these recent experimental advances, the peculiar effects discussed in the present paper may become experimentally accessible in the near future.

In the present paper, we solve the scattering problem for photons in one-dimensional waveguides coupled to a single three-level emitter in various configurations (cf figure 2). It is shown that a waveguide coupled to a V-type emitter or a driven  $\Lambda$ -type emitter

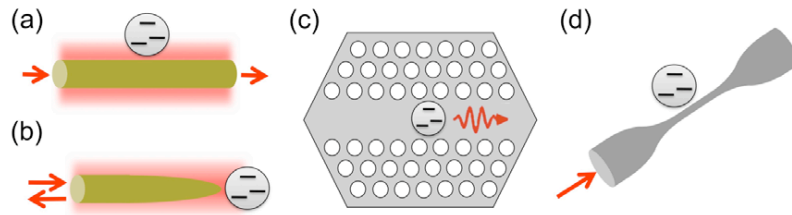


**Figure 1.** Possible experimental realizations of a one-dimensional waveguide strongly coupled to a single emitter: an SPP mode on a metallic nanowire (a) and on a metallic nanotip (b) and a guided mode in a photonic crystal waveguide (c) or a tapered optical fiber (d).

shows a transmission and reflection spectrum characteristic of electromagnetically induced transparency (EIT). Raman scattering occurs for a  $\Lambda$ -type emitter. Most remarkably, the Raman scattering amplitude can be turned to one on resonance, so that the photon is deterministically transferred to a sideband, flipping the quantum state of the emitter. These features allow for a variety of applications in quantum optics and quantum information. A possible realization of a single-photon transistor from a driven emitter is discussed in section 4.1. The transmission through a regular array of emitters is discussed in section 4.2. It is shown that the resulting photonic Bloch bands are widely tunable with an external classical control field. Disorder in the emitter positions leads to Anderson localization of the photonic eigenstates, where the localization length can also be controlled by the external field as shown in section 4.3.

## 2. Single photons in nanoscale waveguides

In this section, we review the scattering problem for a photon in a quasi-one-dimensional geometry coupled to a single quantum emitter as sketched in figure 1. This model was previously studied in [1], [20]–[22] and the transmission coefficient was calculated in [1]. The dynamics is governed by two effects that are usually not present in free space, the strong coupling to a single emitter and the interference of spontaneously emitted waves. In particular, the dynamics in such a one-dimensional waveguide is modeled by the Hamiltonian

$$\hat{H}_{\text{tot}} = \hat{H}_{\text{free}} + \hat{H}_{\text{atom}} + \hat{H}_{\text{int}}. \quad (1)$$

To describe the free propagation of the photons, we will assume that the photons have a linear dispersion relation for the entire frequency range of interest. In reality, many of the structures considered in figure 1 have considerable dispersion and possibly a cut-off in the frequency spectrum. Most emitters, however, only talk to a very narrow frequency interval with a width given by the effective decay rate  $\gamma + \Gamma$  (defined below). For almost any emitter this width is much smaller than the mean frequency  $\omega_0 \gg \gamma + \Gamma$ . Unless there is extremely strong dispersion or one is very close to the cut-off frequency, one can thus safely replace the propagation velocity  $c$  by the group velocity at that frequency. Furthermore, the narrow frequency means that one can safely decompose the field into two distinct contributions with positive and negative wavenumbers, corresponding to right- and left-moving modes. The free propagation of the photons is then described by the Hamiltonian

$$\hat{H}_{\text{free}} = -ic \int dx \hat{a}_{\text{R}}^\dagger(x) \frac{\partial}{\partial x} \hat{a}_{\text{R}}(x) - \hat{a}_{\text{L}}^\dagger(x) \frac{\partial}{\partial x} \hat{a}_{\text{L}}(x), \quad (2)$$

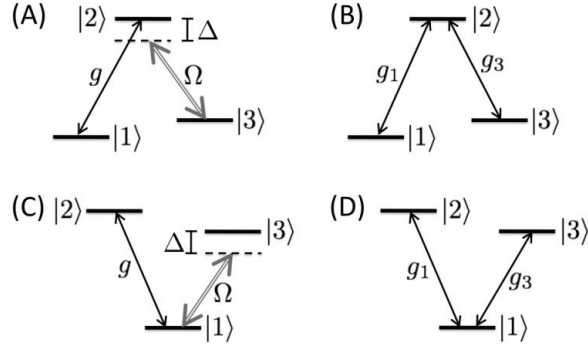


**Figure 2.** The different atomic level schemes considered in the present paper. (a) Electromagnetically induced transparency (EIT) in a driven  $\Lambda$ -system, (b) Raman scattering in a  $\Lambda$ -system, (c) Raman scattering in a driven V-system and (d) electromagnetically induced transparency in a V-system.

where  $\hat{a}_R(x)$  and  $\hat{a}_L(x)$  denote the annihilation operators of a right- or left-moving photon at position  $x$ , respectively.

The interaction Hamiltonian is local at the position of the emitter  $x_0$  and is given by

$$\hat{H}_{\text{int}} = \bar{g} \int dx \delta(x - x_0) \hat{S}_+ (\hat{a}_R(x) + \hat{a}_L(x)) + \text{h.c.}, \quad (3)$$

where  $\hat{S}_-$  and  $\hat{S}_+ = \hat{S}_-^\dagger$  denote atomic lowering and raising operators, respectively, and  $\bar{g}$  denotes the coupling constant. We will consider different structures of the emitter described by different Hamiltonians  $\hat{H}_{\text{atom}}$ , which will be specified for the respective situations below. In the following, we set  $\hbar = 1$ , thus measuring all energies in frequency units. A spatially discretized version of this model was studied in [23]–[26] in the context of coupled optical resonator arrays, which leads to a cosine-shaped dispersion relation. As expected, the photon scattering is very similar in the linear region, whereas significant differences arise in the vicinity of the cut-off frequency.

The dynamics is simplified by setting the coordinates such that  $x_0 = 0$  and introducing the (anti)-symmetric modes

$$\begin{aligned} \hat{a}_e(x) &= \frac{1}{\sqrt{2}} (\hat{a}_R(x) + \hat{a}_L(-x)), \\ \hat{a}_o(x) &= \frac{1}{\sqrt{2}} (\hat{a}_R(x) - \hat{a}_L(-x)), \end{aligned} \quad (4)$$

so that the Hamiltonian for the symmetric mode reads

$$\begin{aligned} \hat{H}_{\text{free}} &= -ic \int dx \hat{a}_e^\dagger(x) \frac{\partial}{\partial x} \hat{a}_e(x), \\ \hat{H}_{\text{int}} &= g \int dx \delta(x) \left( \hat{S}_- \hat{a}_e^\dagger(x) + \hat{S}_+ \hat{a}_e(x) \right), \end{aligned} \quad (5)$$

with  $g = \sqrt{2}\bar{g}$ , while the antisymmetric mode  $\hat{a}_o$  does not couple to the emitter at all. In the following, we will use the symmetric mode for actual calculations and translate the results back afterwards. For calculating the transmission or reflection we will, however, also be interested

in calculating these for a photon traveling along the one-dimensional waveguide. In this case, the solution can easily be found from the solution for the  $e$  mode by expanding the left- and right-going modes on the  $e$  and non-interacting  $o$  mode. Transmission and reflection amplitudes referring to the left- and right-moving modes will be labeled by a tilde to distinguish them from the results for the  $e/o$ -modes. Experimentally the left- and right-moving modes naturally correspond to e.g. sending in the photon from the left or right, whereas a photon incident in the  $e$ -mode corresponds to a photon incident from both sides simultaneously with a suitably chosen phase.

For some systems a more efficient coupling may be realized by placing the emitter at one end of a semi-infinite waveguide instead of side-to-side. This was shown in particular for plasmonic waveguides [16], where the electric field strength around a nanotip is significantly increased (cf figure 1(b)). The propagation of the right- and left-going modes is then restricted to  $x < 0$ . In this case we introduce the mode function

$$\hat{a}_e(x) = \begin{cases} \hat{a}_R(x), & \text{for } x < 0, \\ \hat{a}_L(-x), & \text{for } x > 0, \end{cases} \quad (6)$$

such that  $x < 0$  describes the incoming and  $x > 0$  the reflected photons. The original Hamiltonian (1) then also assumes the form (5) with  $g = \bar{g}$ . For such a semi-infinite structure an incident photon is naturally in mode  $e$ , but if a situation corresponding to the left- and right-moving modes for the one-dimensional waveguide is desired, this can be realized by splitting the incident light on a beam splitter. Placing the semi-infinite structure in one of the output paths and reflecting both paths back to the beam splitter allow one to effectively realize the left- and right-moving modes as the modes incident on the beam splitter.

It is easy to show that the rate of spontaneous emission into the one-dimensional waveguide is given by  $\Gamma = g^2/c$ . Below we mostly use  $\Gamma$  to characterize the interaction strength. Spontaneous emission to other modes out of the one-dimensional waveguide is modeled by attributing an imaginary part  $-i\gamma/2$  to the energies of the excited levels in  $\hat{H}_{\text{atom}}$  in the spirit of the quantum jump picture, where dissipative time evolution is separated into an evolution with such a non-Hermitian Hamiltonian interrupted by random quantum jumps [27, 28]. For our situation the quantum jumps correspond to loss of the photon out of the system by spontaneous emission from the emitter. For calculating the reflection and transmission, we can therefore ignore the quantum jumps and only consider the non-Hermitian Hamiltonian.

The basic scattering problem for one photon interacting with a two-level emitter has been solved by Shen and Fan [1]. In this case, we have  $\hat{H}_{\text{atom}} = (\omega_0 - i\gamma/2)|e\rangle\langle e|$  and  $\hat{S}_+ = \sigma_+$ , where  $\sigma_j$  denotes the respective Pauli matrices. The solution starts from an eigenstate of the full Hamiltonian, which can be written as

$$|\Psi\rangle = \int dx f_g(x) \hat{a}_e^\dagger(x) |g, \emptyset\rangle + f_e |e, \emptyset\rangle, \quad (7)$$

where  $|g\rangle$  and  $|e\rangle$  are the ground and excited states of the emitter, respectively. Here and in the following,  $|\emptyset\rangle$  denotes the state of zero photons, i.e. the empty waveguide. The mode function is discontinuous due to the  $\delta$ -function in the interaction Hamiltonian,

$$f_g(x) = \begin{cases} f_{\text{in}}(x), & \text{for } x < 0, \\ f_{\text{out}}(x), & \text{for } x > 0. \end{cases} \quad (8)$$

Using the Lippmann–Schwinger formalism, one can then rigorously show that an input state given by the mode function  $f_{\text{in}}(x)$  is scattered to an output state given by the mode function

$f_{\text{out}}(x)$  [21]. In particular, one finds that the transmission amplitude for a monochromatic input state with wave number  $k$  is given by [1]

$$t_k = \frac{ck - \omega_0 + i(\gamma - \Gamma)/2}{ck - \omega_0 + i(\gamma + \Gamma)/2}. \quad (9)$$

The scattering problem for a two-photon Fock state can be solved in a similar way [20, 21]. The two photons interact indirectly via the emitter, generating a strongly correlated output state. Numerical results for larger photon numbers are presented in [25, 26].

This procedure can be readily generalized to three-level emitters, which we do below. Some attention, however, has to be paid in the case of two ground states, i.e. a  $\Lambda$ -type atom as shown in figure 2(b).

### 3. Scattering by a three-level atom

In this section, we solve the scattering problem for a single photon and a three-level emitter with three internal states. The different possibilities for the coupling and a classical driving field are sketched in figure 2.

#### 3.1. Electromagnetically induced transparency in a driven $\Lambda$ -system

We start with the driven  $\Lambda$  level scheme shown in figure 2(a), where the excited atomic state  $|2\rangle$  is coupled to another level  $|3\rangle$  by a classical laser beam with Rabi frequency  $\Omega$  and detuning  $\Delta$ . Within the rotating wave approximation, the atomic Hamiltonian is given by

$$H_{\text{atom}} = (E_2 - i\gamma_2/2)|2\rangle\langle 2| + (E_2 - \Delta - i\gamma_3/2)|3\rangle\langle 3| + \frac{\Omega}{2}(|3\rangle\langle 2| + |2\rangle\langle 3|), \quad (10)$$

where we have set the energy scale such that the energy of level  $|1\rangle$  is zero. The interaction Hamiltonian is given by equation (5) with  $\hat{S}_+ = |2\rangle\langle 1|$ . The atomic Hamiltonian  $\hat{H}_{\text{atom}}$  is non-Hermitian, due to the inclusion of the atomic decay to states outside the system as discussed above. In general, such a non-Hermitian Hamiltonian can have complex eigenvalues associated with the resonance eigenstates, which describe the decay of an excitation initially stored in the emitter. In the present paper, however, we are only interested in the scattering continuum with real eigenvalues. Throughout this paper, we assume that the emitter is initially in a ground state and the photon is incident with the (real) energy  $E = ck$ .

The scattering eigenstates of the full Hamiltonian (1) are then given by

$$|E\rangle = \int dx f_1(x) \hat{a}_e^\dagger(x) |\emptyset, 1\rangle + f_2 |\emptyset, 2\rangle + f_3 |\emptyset, 3\rangle \quad (11)$$

with eigenenergy  $E = ck$ . The coefficients are easily found to be

$$\begin{aligned} f_1(x) &= \frac{1}{\sqrt{2\pi}} (\Theta(-x) + t_k \Theta(+x)) e^{ikx}, \\ f_2 &= \frac{1}{\sqrt{2\pi}} \frac{ic(t_k - 1)}{\sqrt{c\Gamma}}, \\ f_3 &= \frac{1}{\sqrt{2\pi}} \frac{ic\Omega(t_k - 1)}{2(ck + \Delta)}, \end{aligned} \quad (12)$$

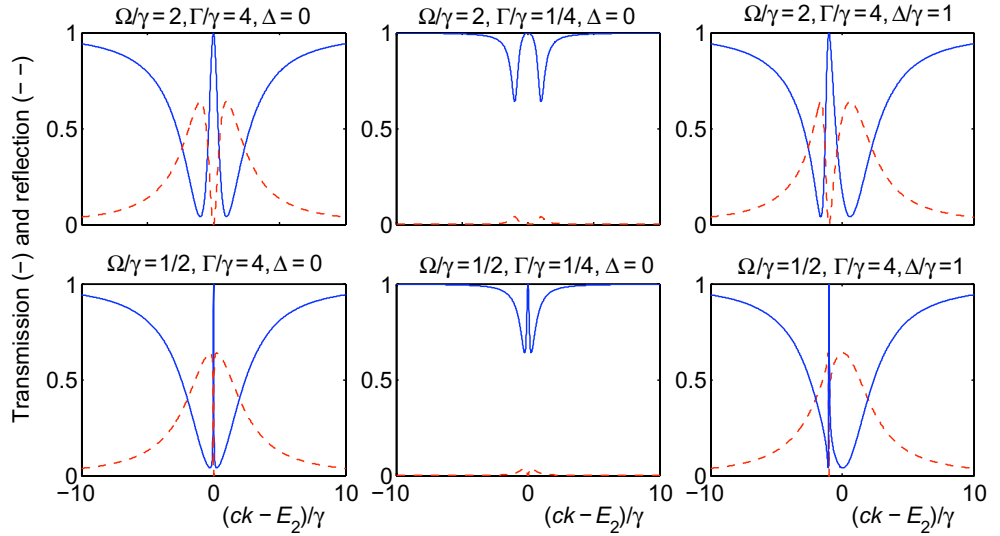


**Figure 3.** Transmission (solid line) and reflection (dashed line) spectra of the driven  $\Lambda$ -type atom for different values of the parameters  $\Omega$ ,  $\Gamma$  and  $\Delta$ .

where the transmission coefficient is given by

$$t_k = \frac{[ck - (E_2 - \Delta - i\gamma_3/2)][ck - (E_2 - i\gamma_2/2) - i\Gamma/2] - \Omega^2/4}{[ck - (E_2 - \Delta - i\gamma_3/2)][ck - (E_2 - i\gamma_2/2) + i\Gamma/2] - \Omega^2/4} \quad (13)$$

and  $\Theta(x)$  denotes the Heaviside step function. An incoming photon with wave number  $k$  in the  $e$ -mode thus experiences a phase shift given by  $t_k$  when it crosses the atom. The modulus of  $t_k$  is smaller than one for  $\gamma_2 > 0$  or  $\gamma_3 > 0$ , which describes transversal losses, i.e. the scattering of the photon out of the waveguide. In this case, the emitter jumps incoherently to one of the ground levels and the photon is lost.

Let us first consider the case where level  $|3\rangle$  is metastable, i.e.  $\gamma_3 = 0$ . This situation is realized, for example, when the levels  $|1\rangle$  and  $|3\rangle$  are two hyperfine states in the ground state manifold. Going back to left- and right-moving modes using equation (4), one finds that the transmission and reflection amplitudes of the waveguide are given by

$$\tilde{t}_k = \frac{t_k + 1}{2} \quad \text{and} \quad \tilde{r}_k = \frac{t_k - 1}{2}. \quad (14)$$

The resulting transmission spectrum is depicted in figure 3 for different values of the parameters  $\Omega$ ,  $\Delta$  and  $\Gamma$ , showing the familiar EIT transmission spectrum [29]. The atom becomes fully transparent on two-photon resonance, i.e. when the wave number is given by

$$ck = E_2 - \Delta. \quad (15)$$

The width of this central transparency window is only determined by the strength of the driving field  $\Omega$ . Furthermore, the system is transparent for  $(ck - E_2) \rightarrow \pm\infty$ , where the incoming photon is far off-resonant and thus does not interact with the atom. In between, we find dips of the transmission, whose width and depth increase with the coupling strength  $\Gamma$ . These are mainly due to reflection if  $\Gamma > \gamma$  and due to losses otherwise. Complete reflection is only possible if the losses vanish exactly ( $\gamma = 0$ ) and

$$ck = E_2 - \frac{\Delta}{2} \pm \frac{\Omega_{\text{eff}}}{2}, \quad (16)$$

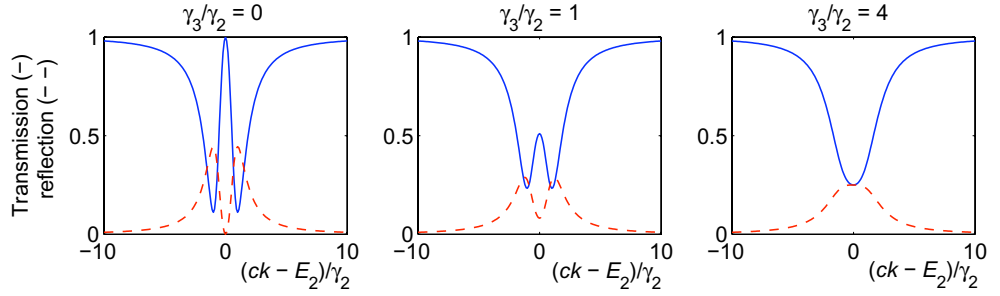


**Figure 4.** Transmission (solid line) and reflection (dashed line) spectra of the driven  $\Lambda$ -type atom for different values of  $\gamma_3$ . The remaining parameters are chosen to be  $\Omega/\gamma_2 = 2$ ,  $\Gamma/\gamma_2 = 2$  and  $\Delta = 0$ .

where  $\Omega_{\text{eff}} = (\Omega^2 + \Delta^2)^{1/2}$  denotes the effective Rabi frequency. The complete spectrum is symmetric only for  $\Delta = 0$  and asymmetric otherwise.

The waveguide can be fully transparent only if level  $|3\rangle$  is metastable. For  $\gamma_3 > 0$  there will always be losses such that  $|\tilde{t}_k|^2 + |\tilde{r}_k|^2 < 1$ . Figure 4 shows how the transmission spectrum changes when  $\gamma_3$  is increased: the transmission on resonance decreases until finally the EIT transparency window vanishes completely.

### 3.2. A $\Lambda$ -system with two coupling transitions

The  $\Lambda$ -system shown in figure 2(b), where both ground states couple to the waveguide mode, is described by the atomic Hamiltonian

$$H_{\text{atom}} = E_1|1\rangle\langle 1| + E_3|3\rangle\langle 3| + (E_2 - i\gamma/2)|2\rangle\langle 2|$$

and the interaction Hamiltonian

$$H_{\text{int}} = \int dx \delta(x) [g_1 \hat{a}_e^\dagger(x)|1\rangle\langle 2| + g_3 \hat{a}_e^\dagger(x)|3\rangle\langle 2| + \text{h.c.}]. \quad (17)$$

Now, we have to take into account that the atom can be in either state  $|1\rangle$  or  $|3\rangle$  when a photon is present. An arbitrary state with one excitation can thus be written as

$$|\Psi\rangle = \int dx [f_1(x) \hat{a}_e^\dagger(x)|\emptyset, 1\rangle + f_3(x) \hat{a}_e^\dagger(x)|\emptyset, 3\rangle] + f_2|\emptyset, 2\rangle. \quad (18)$$

The eigenstates of the full Hamiltonian are found by substituting this ansatz into the time-independent Schrödinger equation. Then one finds two types of solution.

The continuous solution is a ‘dark state’ characterized by destructive interference of the functions  $f_1(x)$  and  $f_3(x)$  at the position of the atom so that this mode does not interact. The solution is thus given by

$$\begin{aligned} f_1(x) &= \mathcal{N} g_3 e^{ik_1 x}, \\ f_3(x) &= -\mathcal{N} g_1 e^{ik_3 x}, \\ f_2 &= 0 \end{aligned} \quad (19)$$

with the normalization factor  $\mathcal{N} = (2\pi(g_1^2 + g_3^2))^{-1/2}$ . The wave numbers are related to the eigenenergy by  $ck_1 = E - E_1$  and  $ck_3 = E - E_3$ .

The other solution is discontinuous due to the interaction with the atom. One finds that

$$\begin{aligned} f_1(x) &= \mathcal{N} g_1 [\Theta(-x) + t_E \Theta(x)] e^{ik_1 x}, \\ f_3(x) &= \mathcal{N} g_3 [\Theta(-x) + t_E \Theta(x)] e^{ik_3 x}, \\ f_2 &= ic(t_k - 1), \end{aligned} \quad (20)$$

with the transmission coefficient

$$t_E = \frac{(E - E_2 + i\gamma/2) - i(\Gamma_1 + \Gamma_3)/2}{(E - E_2 + i\gamma/2) + i(\Gamma_1 + \Gamma_3)/2}, \quad (21)$$

where  $\Gamma_j = g_j^2/2$  are the spontaneous emission rates into the waveguide when the emitter decays into the respective atomic level.

Using these states, one can easily solve the scattering problem. We find that an incoming photon with wave number  $k$  is scattered depending on the atomic state according to

$$\begin{aligned} |k, 1\rangle_e &\rightarrow \frac{t_E \Gamma_1 + \Gamma_3}{\Gamma_1 + \Gamma_3} |k, 1\rangle_e + \frac{\sqrt{\Gamma_1 \Gamma_3} (t_E - 1)}{\Gamma_1 + \Gamma_3} |k - q, 3\rangle_e \\ &\quad \text{with } E = E_1 + ck, \\ |k, 3\rangle_e &\rightarrow \frac{\Gamma_1 + t_E \Gamma_3}{\Gamma_1 + \Gamma_3} |k, 3\rangle_e + \frac{\sqrt{\Gamma_1 \Gamma_3} (t_E - 1)}{\Gamma_1 + \Gamma_3} |k + q, 1\rangle_e \\ &\quad \text{with } E = E_3 + ck, \end{aligned} \quad (22)$$

where  $cq = (E_3 - E_1)$  is the energy difference between the two ground states.

A remarkable result is that a resonant photon in mode  $e$  can be absorbed deterministically as pointed out in [2] for the case  $\gamma = 0$ . Suppose the emitter is initially prepared in the ground state  $|1\rangle$  and the coupling constants satisfy the condition  $\Gamma_1^2 - \Gamma_3^2 = \gamma(\Gamma_1 + \Gamma_3)$ . The transmission amplitude is then given by  $t_E = -\Gamma_3/\Gamma_1$  and the internal state of the emitter is flipped,

$$|k, 1\rangle_e \rightarrow -\sqrt{\Gamma_3/\Gamma_1} |k - q, 3\rangle_e, \quad (23)$$

as long as the photon is not lost. If transversal losses are absent, i.e.  $\gamma = 0$ , the scattering process realizes a deterministic quantum gate between a photon and a single emitter. However, the described protocol is also very useful in the case  $\gamma \neq 0$ , when a significant fraction of the incident photons is lost. If a single photon is measured in the output, the gate is known to have operated successfully. Combined with error-proof quantum communication schemes [30]–[32], this provides a powerful building block for quantum computing purposes. We will discuss the realization of a single-photon transistor using this property in section 4.1.

### 3.3. Driven V-type atom

Next we consider the situation shown in figure 2(c), where the classical driving field couples the ground state  $|1\rangle$  to the excited state  $|3\rangle$ , so that the atomic Hamiltonian is now given by

$$H_{\text{atom}} = (E_2 - i\gamma/2)|2\rangle\langle 2| - \Delta|3\rangle\langle 3| + \frac{\Omega}{2}(|3\rangle\langle 1| + |1\rangle\langle 3|). \quad (24)$$

The interaction Hamiltonian is given by equation (5) with  $\hat{S}_+ = |2\rangle\langle 1|$ . The state  $|3\rangle$  is assumed to be stable: for instance, the states  $|1\rangle$  and  $|3\rangle$  can be two hyperfine states coupled by microwave radiation.

The situation is best dealt with in a dressed state picture, introducing the eigenstates of the atomic Hamiltonian

$$\begin{aligned} |+\rangle &= \frac{1}{\sqrt{2\Omega_{\text{eff}}(\Omega_{\text{eff}} - \Delta)}} (\Omega|1\rangle + (\Omega_{\text{eff}} - \Delta)|3\rangle), \\ |-\rangle &= \frac{1}{\sqrt{2\Omega_{\text{eff}}(\Omega_{\text{eff}} + \Delta)}} (\Omega|1\rangle - (\Omega_{\text{eff}} + \Delta)|3\rangle) \end{aligned} \quad (25)$$

with eigenenergies

$$E_{\pm} = -\frac{\Delta}{2} \pm \frac{\Omega_{\text{eff}}}{2}. \quad (26)$$

The atomic and interaction Hamiltonians are then given by

$$\begin{aligned} H_{\text{atom}} &= E_+|+\rangle\langle +| + E_-|-\rangle\langle -| + (E_2 - i\gamma/2)|2\rangle\langle 2|, \\ H_{\text{int}} &= \int dx \delta(x) \hat{a}_e^\dagger(x) [g_+|+\rangle\langle 2| + g_- \hat{a}_e^\dagger(x)|-\rangle\langle 2| + \text{h.c.}]. \end{aligned} \quad (27)$$

with

$$g_{\pm} = \frac{g\Omega}{\sqrt{2\Omega_{\text{eff}}(\Omega_{\text{eff}} \mp \Delta)}}. \quad (28)$$

This is exactly the situation depicted in figure 2(b), which has been discussed in the previous section. However, a driven system has the enormous advantage that system parameters such as the ratio  $g_+/g_-$  can be tuned to almost any desired value by choosing an appropriate classical control field. In particular, this can be used to implement a single-photon transistor as shown in section 4.1.

Using the result from the previous section, one finds that an incoming photon with wave number  $k$  is scattered according to

$$\begin{aligned} |k, +\rangle_e &\rightarrow \frac{t_E \Gamma_+ + \Gamma_-}{\Gamma_+ + \Gamma_-} |k, +\rangle_e + \frac{\sqrt{\Gamma_+ \Gamma_-} (t_E - 1)}{\Gamma_+ + \Gamma_-} |k - q, -\rangle_e \\ &\quad \text{with } E = E_+ + ck - E_2, \\ |k, -\rangle_e &\rightarrow \frac{\Gamma_+ + t_E \Gamma_-}{\Gamma_+ + \Gamma_-} |k, -\rangle_e + \frac{\sqrt{\Gamma_+ \Gamma_-} (t_E - 1)}{\Gamma_+ + \Gamma_-} |k + q, +\rangle_e \\ &\quad \text{with } E = E_- + ck - E_2, \end{aligned} \quad (29)$$

where  $cq = (E_- - E_+)$  is the energy difference between the two dressed states and  $\Gamma_{\pm} = g_{\pm}^2/c$  as above. The transmission phase factor is given by

$$t_E = \frac{(E - E_2 + i\gamma/2) - i(\Gamma_+ + \Gamma_-)/2}{(E - E_2 + i\gamma/2) + i(\Gamma_+ + \Gamma_-)/2}. \quad (30)$$

### 3.4. A V-type atom with two coupling transitions

This case, depicted in figure 2(d), is equivalent to case A in the dressed state picture as long as loss can be neglected. In the general case, one has to be a bit more careful, because the loss terms are also changed by a transformation to the dressed state basis. In the following, we therefore give the full solution for the case of a V-type atom with two coupling transitions.

We consider the atomic Hamiltonian

$$H_{\text{atom}} = (E_2 - i\gamma_2/2)|2\rangle \langle 2| + (E_3 - i\gamma_3/2)|3\rangle \langle 3|, \quad (31)$$

where we have set the energy scale such that the energy of level  $|1\rangle$  is zero. The interaction Hamiltonian is given by

$$\hat{H}_{\text{int}} = \int dx \delta(x) (g_2 \hat{a}_e(x)|2\rangle \langle 1| + g_3 \hat{a}_e(x)|3\rangle \langle 1| + \text{h.c.}). \quad (32)$$

The eigenstates of the full Hamiltonian can then be written

$$|E\rangle = \int dx f_1(x) \hat{a}_e^\dagger(x) |\emptyset, 1\rangle + f_2 |\emptyset, 2\rangle + f_3 |\emptyset, 3\rangle \quad (33)$$

with eigenenergy  $E = ck$ . The coefficients are easily found to be

$$\begin{aligned} f_1(x) &= \frac{1}{\sqrt{2\pi}} (\Theta(-x) + t_k \Theta(+x)) e^{ikx}, \\ f_2 &= \frac{1}{2\sqrt{2\pi}} \frac{\sqrt{c\Gamma_2}(1+t_k)}{ck - E_2 + i\gamma_2/2}, \\ f_3 &= \frac{1}{2\sqrt{2\pi}} \frac{\sqrt{c\Gamma_3}(1+t_k)}{ck - E_3 + i\gamma_3/2}, \end{aligned}$$

where the transmission coefficient is given by

$$t_k = \frac{[ck - (E_2 - i\gamma_2/2) - i\Gamma_2/2][ck - (E_3 - i\gamma_3/2) - i\Gamma_3/2] + \Gamma_2\Gamma_3/4}{[ck - (E_2 - i\gamma_2/2) + i\Gamma_2/2][ck - (E_3 - i\gamma_3/2) + i\Gamma_3/2] + \Gamma_2\Gamma_3/4}. \quad (34)$$

An incoming photon with wave number  $k$  in the  $e$ -mode thus experiences a phase shift given by  $t_k$  when it crosses the atom. The reflection ( $\tilde{r}_k$ ) and transmission ( $\tilde{t}_k$ ) amplitudes for the left- and right-moving modes are again given by equation (14). The atom is fully reflective if one of the levels  $|2\rangle$  or  $|3\rangle$  is metastable and the photon is resonant to the atomic transition between the metastable and the ground level:

$$|\tilde{r}_k| = 1 \quad \text{for} \quad \begin{cases} ck = E_2 & \text{and} & \gamma_2 = 0 \\ ck = E_3 & \text{and} & \gamma_3 = 0. \end{cases} \quad \text{or} \quad (35)$$

It can become fully transparent only if both excited states are metastable:

$$|\tilde{t}_k| = 1 \quad \text{if} \quad \frac{ck - E_2}{ck - E_3} = \frac{\Gamma_2}{\Gamma_3} \quad \text{and} \quad \gamma_2 = \gamma_3 = 0. \quad (36)$$

## 4. Applications

Having solved the basic scattering problem, we now go on to discuss various applications of these results.

### 4.1. A single-photon transistor

A single-photon transistor is a universal nonlinear element with wide-ranging application from classical telecommunication to quantum computing [22, 33]. However, it is very hard to realize

since photons rarely interact directly, so that the necessary interactions must be mediated by matter in a deterministic way.

The basic idea of this transistor is that a waveguide strongly coupled to a single emitter is either reflective or transparent, depending on the state of the emitter. The state can then be switched by a single gate photon. Previously, a realization of such a device in nanoscale one-dimensional waveguides has been proposed [22]. A disadvantage of this method is that it requires a precise timing between the quantum gate photon and a classical control pulse. Here we present an alternative approach that removes this restriction.

This single-photon transistor works as follows: consider the situation sketched in figure 2(c), whose scattering properties have been analyzed in section 3.3. Initially the system is in state  $|1\rangle$  and the classical control field is off  $\Omega(-\infty) = 0$ . Now the emitter is driven to the state  $|+\rangle$  by an adiabatic passage technique, slowly increasing  $\Omega$  and possibly varying the driving frequency so that finally a situation with  $\Omega \neq 0$  and  $\Delta = 0$  is reached. Several methods for this procedure were demonstrated experimentally (see e.g. [34]). After this initialization procedure, the transistor is sensitive to the arrival of the gate photon as long as the driving field remains on. If the gate photon is injected in mode  $e$ , it scatters according to equation (29). As we have prepared the emitter such that  $\Delta = 0$  we have  $\Gamma_+ = \Gamma_- = \Gamma/2$ . Assuming that the photon is resonant,  $ck = E_2 - E_+$ , the transmission coefficient is given by  $t_E = -1$  as long as losses can be neglected. Thus, the internal state of the emitter is changed during the scattering process according to

$$\text{gate photon present: } |k, +\rangle \rightarrow -|k, -\rangle,$$

$$\text{no gate photon: } |k, +\rangle \rightarrow |k, +\rangle.$$

After the scattering process, the initialization sequence is reversed, mapping  $|+\rangle$  back to  $|1\rangle$  and  $|-\rangle$  to  $|3\rangle$ . Thus the state of the emitter is switched from  $|1\rangle$  to  $|3\rangle$  if and only if a gate photon has crossed the waveguide. As the external field is now switched off,  $\Omega = 0$ , the scattering is essentially that of a two-level emitter. As shown in [1], the waveguide is then completely reflective for photons moving left or right if the emitter is in state  $|1\rangle$ . On the other hand, if it has been switched to state  $|3\rangle$  by the gate photon, it is essentially decoupled—the waveguide is transparent. This procedure therefore implements a single-photon transistor, where the transmission of a large number of photons may be controlled by the presence or absence of a single-gate photon. It should be noted that this procedure does not need a precise timing. The initialization and de-initialization sequences must be performed well before and well after the gate photon passes, but the precise time does not play a role. Furthermore, the de-initialization is performed by an adiabatic passage, which is typically more robust than procedures relying on Rabi flopping.

In the description of the basic idea, we neglected losses and assumed a perfect resonance. Let us now consider a more realistic situation and calculate the switching probability for a general input state

$$|\Psi_{\text{in}}\rangle = \int dk f(k) a_{e,k}^\dagger |+\rangle, \quad (37)$$

In particular, we consider a Gaussian input pulse

$$f(k) = \frac{1}{\sqrt{2\pi}\sigma} e^{-(ck-\omega_0)^2/4\sigma^2}, \quad (38)$$

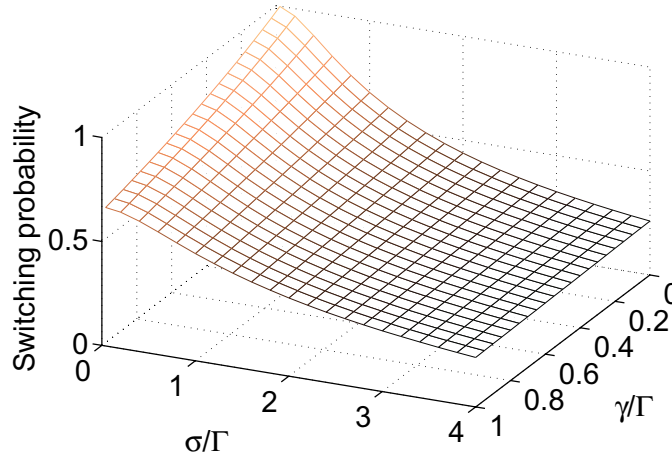


**Figure 5.** Switching probability of the single-photon transistor described in the text as a function of the loss rate  $\gamma$  and the frequency width of the incident photon  $\sigma$  for  $\Delta = 0$ .

at resonance with the transition  $\omega_0 = E_2 - E_+$ . Assuming that the adiabatic passage to the dressed state works perfectly, the switching probability is then given by the probability to find the emitter in state  $|-\rangle$  after the scattering:

$$p_s = \int |f(k)|^2 \frac{|t_E - 1|^2}{4} dk + \int |f(k)|^2 \frac{1 - |t_E|^2}{4} dk. \quad (39)$$

The first term gives the norm of the contribution of  $|-\rangle$  in the scattering state (29), weighted by the pulse shape of the gate photon and using  $\Gamma_+ = \Gamma_-$ . The second contribution is the probability that the emitter decays to level  $|-\rangle$  when the gate photon is lost by spontaneous emission to the outside world, where the branching ratio is  $1/2$ . In figure 5, the switching probability is plotted for the case  $\Delta = 0$  as a function of the width of the input pulse  $\sigma$  and the loss rate  $\gamma$ .

#### 4.2. Tunable photonic band gaps

Let us now consider the properties of a periodic array of emitters (cf figure 6), which can be realized for instance using a fiber-based atom trap [12]. The emitters are driven by a classical laser field in the EIT configuration shown in figure 2(a). The strength and detuning of this driving then allows us to tune the transport properties of the array.

Let us first consider the lossless case  $\gamma_2 = \gamma_3 = 0$ . The amplitudes of the right- and left-going waves in this array are then related by

$$\begin{pmatrix} a_{R,n+1} \\ a_{L,n+1} \end{pmatrix} = T \begin{pmatrix} a_{R,n} \\ a_{L,n} \end{pmatrix}, \quad (40)$$

where

$$T = \begin{pmatrix} e^{i\omega d/c} & 0 \\ 0 & e^{-i\omega d/c} \end{pmatrix} \begin{pmatrix} 1/\tilde{t}^* & -\tilde{r}^*/\tilde{t}^* \\ -\tilde{r}/\tilde{t} & 1/\tilde{t} \end{pmatrix} \quad (41)$$

is the transfer matrix (cf [35]). Here,  $d$  denotes the periodicity of the emitter array and the transmission and reflection coefficients defined in equation (14) have been used.

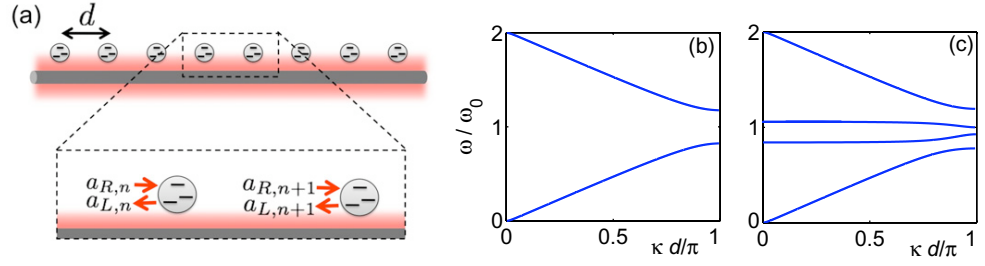


**Figure 6.** (a) Waveguide coupled to a periodic array of emitters in the EIT configuration (cf figure 2(a)). (b) Photonic Bloch bands of the waveguide without driving for  $\Gamma = 0.1\omega_0$  and  $d = 0.5\lambda_0$ , where  $\omega_0 = (E_2 - E_1)$  is the resonance frequency and  $\lambda_0 = 2\pi c/\omega_0$ . (c) Driving the emitters with a Rabi frequency of  $\Omega/\omega_0 = 0.2$  and  $\Delta = 0.1\omega_0$  leads to a splitting of the states around the resonance frequency and the occurrence of new sub-bands.

The eigenvalues of the transfer matrix characterize the transport properties of the array. Since the product of both eigenvalues is always one, the eigenvalues are either complex conjugate numbers of magnitude one ( $e^{\pm i\kappa d}$ ) or they are inverse of each other with magnitudes smaller and larger than one. The first case characterizes a photonic Bloch state with quasi-momentum  $\kappa$ , so that transport is possible. In the latter case, transport is impossible, i.e.  $\omega$  lies in a band gap.

Examples of the resulting photonic Bloch bands  $\omega(\kappa)$  are shown in figure 6. For  $\Omega = 0$  (no driving), one recovers the Bloch bands well known for simple two-level emitters [1], with a band gap at the resonance frequency. For  $\Omega > 0$ , however, the upper level splits into two dressed states, which both give rise to a Bloch band. The position and width of these bands are then tunable through  $\Omega$  and  $\Delta$ .

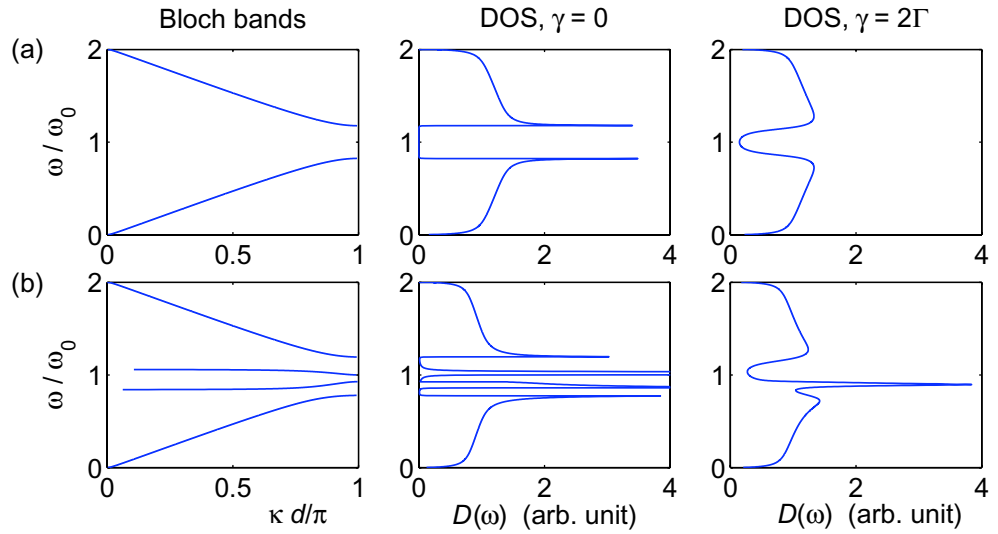
In a realistic system, the coupling to the waveguide will not be perfect and transversal losses by spontaneous decay from the excited state  $|2\rangle$  cannot be neglected. Then the transfer matrix is no longer unitary and its eigenvalues are rather given by  $e^{\sigma d} e^{\pm i\kappa d}$ , where  $\sigma$  gives the absorption coefficient. The effect of losses on the photonic band gap structure is illustrated in figure 7, where we compare the density of states  $D(\omega)$  with and without transversal losses. In the lossless case, the density of states  $D(\omega)$  is essentially given by  $(d\omega/d\kappa)^{-1}$ . For  $\gamma \neq 0$ , every state is broadened, so that the density of states is rather given by

$$\begin{aligned} D(\omega') &= \int d\kappa |\chi(\kappa)|^2 \frac{\sigma(\kappa)/2\pi}{(\omega(\kappa) - \omega')^2 + \sigma\kappa^2} \\ &= \int d\omega |\chi(\omega)|^2 \left(\frac{d\omega}{d\kappa}\right)^{-1} \frac{\sigma(\omega)/2\pi}{(\omega - \omega')^2 + \sigma(\omega)^2}. \end{aligned} \quad (42)$$

This definition of the density of states is adapted to the modification of the spontaneous emission rate of a single emitter in a photonic crystal structure [36]. Here,  $\chi(\kappa)$  denotes the coupling matrix element of the emitter to a Bloch state with quasi-momentum  $\kappa$ . As the interaction with the waveguide is local at the position  $x_0$  of the emitter (cf equation (3)), the coupling is simply given by the magnitude of the Bloch wave function at the position  $x_0$ :

$$\chi(\kappa) = a_{R,\kappa} e^{i\omega x_0/c} + a_{L,\kappa} e^{-i\omega x_0/c}. \quad (43)$$

In the following example, we chose  $x_0 = d/2$ , i.e. we consider the emission of a single impurity atom placed in the middle between two emitters forming the photonic band gap structure.



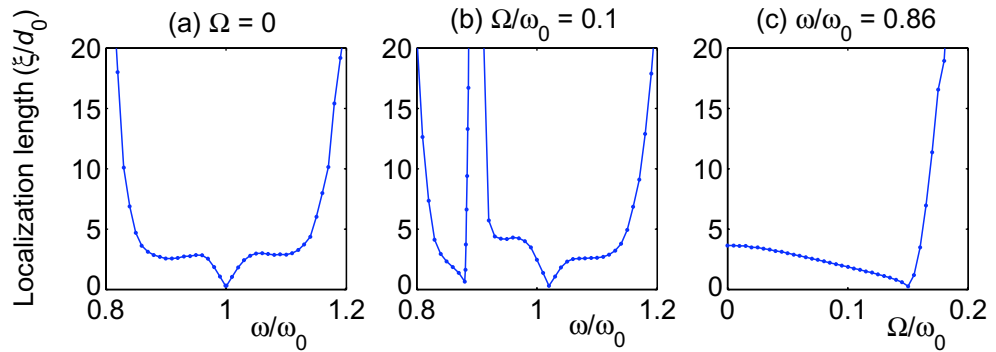
**Figure 7.** Photonic Bloch bands for the same parameters as in figure 6 without (a) and with (b) external driving field. The driving leads to a splitting of Bloch states around the resonance frequency and thus leads to a drastic modification of the density of states (DOS). These features are still very pronounced in the case of strong transversal losses, i.e. large values of  $\gamma$ .

Figure 7 shows that the density of states around the resonance frequency  $\omega_0$  is strongly modified around the resonance frequency  $\omega_0$  by the external driving field. These features are still very pronounced in the case of strong transversal losses, i.e. large values of  $\gamma$ . This can be utilized, for instance, to manipulate the emission rate of a single impurity atom coupled to the waveguide simply by tuning the strength  $\Omega$  of the external driving laser (cf [36, 37]).

#### 4.3. Tunable Anderson localization of photons

In the previous section, we considered transport of photons through a waveguide coupled to an array of emitters in a perfectly periodic configuration. If this periodicity is disturbed by disorder, as it will commonly be in real experiments, there are generally no infinitely extended Bloch states any more. Instead, every photonic wave function undergoes Anderson localization [38]. This localization was demonstrated experimentally in different systems [39, 40]. The localization transition is well understood for systems described by transfer matrices [35] such as (41). Here we consider an array of emitters where the distance between the emitters  $d_n$  differs from site to site, in particular assuming a uniform distribution in the interval  $[0.4, 0.6] \times \lambda_0$ , where  $\lambda_0$  is the free-space wavelength of a photon with frequency  $\omega_0$ . The transfer matrix of a whole array of  $N$  emitters is then given by the product  $T_N = \prod_{j=1}^N T_j$  and its eigenvalues can be written as  $e^{\pm Nd_0/\xi}$ . The localization length  $\xi$  characterizes the spatial extent of a photonic wave function and measures the localization strength.

An example is shown in figure 8 for an array of three-level emitters in the EIT configuration as shown in figure 2(a). We restrict ourselves to the lossless case and set  $\Gamma = 0.1\omega_0$ , where  $\omega_0 = (E_2 - E_1)$  is the atomic resonance frequency. The localization length  $\xi$  is plotted as



**Figure 8.** Photonic Anderson localization in a waveguide strongly coupled to an array of emitters at random positions. (a) Localization length for an array of three-level emitters with parameters  $\Gamma = 0.1\omega_0$  and average emitter distance  $\bar{d} = 0.5\lambda_0$ , where  $\omega_0 = (E_2 - E_1)$  is the resonance frequency and  $\lambda_0 = 2\pi c/\omega_0$ . (b) Driving the emitter with the Rabi frequency  $\Omega/\omega_0 = 0.1$  and  $\Delta/\omega_0 = 0.1$  alters the localization properties fundamentally. (c) Localization length as a function of the strength of the external driving field for  $\omega/\omega_0 = 0.86$ .

a function of the frequency  $\omega$  of the incoming photons as obtained from a Monte Carlo simulation. The transfer matrix  $T_N$  has been computed using  $N = 100$  randomly chosen values for the distance  $d_n$  and diagonalized. The obtained values for the localization constant  $\xi^{-1}$  have been averaged over 100 realizations. Without external driving (figure 8(a)), one observes the localization spectrum of a single two-level emitter. On resonance all emitters are completely reflective so that the localization length tends to zero. The introduction of a classical driving field changes the localization properties dramatically (cf figure 8(b)). The upper state splits into two dressed states, so that there are two resonance frequencies for which the emitters are fully reflective and hence  $\xi = 0$ . On the other hand,  $\xi$  becomes infinite when the EIT condition is fulfilled, as all emitters are fully transparent then.

## 5. Conclusion and outlook

In the present paper, we have solved the scattering problem for a single photon in a one-dimensional waveguide coupled to a three-level emitter. Several different configurations were taken into account. Electromagnetically induced transparency is observed for a driven  $\Lambda$ -system and V-system if both transitions couple to the waveguide. On the contrary, scattering to sidebands occurs for a driven V-system and  $\Lambda$ -system with two coupling transitions.

The control gained by the classical driving field paves the way for a variety of applications from classical optics to quantum information. The control over the transmission in the EIT scheme can be used to tailor the optical properties of an array of emitters. Thus one can readily engineer photonic band gap structures or tune the localization length in disordered systems. The driven V-system can be applied in a single-photon transistor. The gate photon is scattered to a sideband, changing the internal state of the emitter and thus switching the waveguide from reflective to transmissive.

## Acknowledgments

The financial support of the Deutsche Forschungsgemeinschaft via a research fellowship program (grant number WI 3415/1) and the Villum Kann Rasmussen Foundation is gratefully acknowledged.

## References

- [1] Shen J T and Fan S 2005 *Opt. Lett.* **30** 2001
- [2] Pinotsi D and Imamoglu A 2008 *Phys. Rev. Lett.* **100** 093603
- [3] Zumofen G, Mojarad N M, Sandoghdar V and Agio M 2008 *Phys. Rev. Lett.* **101** 180404
- [4] Thompson R J, Rempe G and Kimble H J 1992 *Phys. Rev. Lett.* **68** 1132
- [5] Brune M, Schmidt-Kaler F, Maali A, Dreyer J, Hagley E, Raimond J M and Haroche S 1996 *Phys. Rev. Lett.* **76** 1800
- [6] Reithmaier J P, Sek G, Löffler A, Hofmann C, Kuhn S, Reitzenstein S, Keldysh L V, Kulakovskii V D, Reinecke T L and Forchel A 2004 *Nature* **432** 197
- [7] Yoshie T, Scherer A, Hendrickson J, Khitrova G, Gibbs H M, Rupper G, Ell C, Shchekin O B and Deppe D G 2004 *Nature* **432** 200
- [8] Faraon A, Waks E, Englund D, Fushman I and Vučković J 2007 *Appl. Phys. Lett.* **90** 073102
- [9] Claudon J, Bleuse J, Malik N S, Bazin M, Jaffrennou P, Gregersen N, Sauvan C, Lalanne P and Gérard J-M 2010 *Nat. Photonics* **4** 174
- [10] Babinec T M, Hausmann B J M, Khan M, Zhang Y, Maze J R, Hemmer P R and Lončar M 2010 *Nat. Nanotechnol.* **5** 195
- [11] Dayan B, Parkins A S, Aoki T, Ostby E P, Vahala K J and Kimble H J 2008 *Science* **319** 1062
- [12] Vetsch E, Reitz D, Sague G, Schmidt R, Dawkins S R and Rauschenbeutel A 2010 arXiv:0912.1179
- [13] Bajcsy M, Hofferberth S, Balic V, Peyronel T, Hafezi M, Zibrov A S, Vuletic V and Lukin M D 2009 *Phys. Rev. Lett.* **102** 203902
- [14] Astafiev O, Zagoskin A M, Abdumalikov A Jr, Pashkin Y A, Yamamoto T, Inomata K, Nakamura Y and Tsai J S 2010 *Science* **327** 840
- [15] Chang D E, Sørensen A S, Hemmer P R and Lukin M D 2006 *Phys. Rev. Lett.* **97** 053002
- [16] Chang D E, Sørensen A S, Hemmer P R and Lukin M D 2007 *Phys. Rev. B* **76** 035420
- [17] Akimov A V, Mukherjee A, Yu C L, Chang D E, Zibrov A S, Hemmer P R, Park H and Lukin M D 2007 *Nature* **450** 402
- [18] Hakala T K, Toppari J J, Kuzyk A, Pettersson M, Tikkanen H, Kunttu H and Törmä P 2009 *Phys. Rev. Lett.* **103** 053602
- [19] Hwang J, Pototschnig M, Lettow R, Zumofen G, Renn A, Götzinger S and Sandoghdar V 2009 *Nature* **460** 76
- [20] Shen J T and Fan S 2007 *Phys. Rev. Lett.* **98** 153003
- [21] Shen J T and Fan S 2007 *Phys. Rev. A* **76** 062709
- [22] Chang D E, Sørensen A S, Demler E A and Lukin M D 2007 *Nat. Phys.* **3** 807
- [23] Zhou L, Gong Z R, Liu Y X, Sun C P and Nori F 2008 *Phys. Rev. Lett.* **101** 100501
- [24] Shi T and Sun C P 2009 *Phys. Rev. B* **79** 205111
- [25] Longo P, Schmitteckert P and Busch K 2009 *J. Opt. A: Pure Appl. Opt.* **11** 114009
- [26] Longo P, Schmitteckert P and Busch K 2010 *Phys. Rev. Lett.* **104** 023602
- [27] Dalibard J, Castin Y and Mølmer K 1992 *Phys. Rev. Lett.* **68** 580
- [28] Carmichael H J 1993 *An Open Systems Approach to Quantum Optics (Lecture Notes in Physics)* (Berlin: Springer)
- [29] Fleischhauer M, Imamoglu A and Marangos J P 2005 *Rev. Mod. Phys.* **77** 633
- [30] van Enk S J, Cirac J I and Zoller P 1997 *Phys. Rev. Lett.* **78** 4293

- [31] Sørensen A and Mølmer K 1998 *Phys. Rev. A* **58** 2745
- [32] Witthaut D, Lukin M D and Sørensen A 2010 in preparation
- [33] Bouwmeester D, Ekert A and Zeilinger A (ed) 2000 *The Physics of Quantum Information* (Berlin: Springer)
- [34] Oberst M, Klein J and Halfmann T 2006 *Opt. Commun.* **264** 463
- [35] Berry M V and Klein S 1997 *Eur. J. Phys.* **18** 222
- [36] Yablonovitch E 1987 *Phys. Rev. Lett.* **58** 2059
- [37] Lodahl P, van Driel A F, Nikolaev I S, Irman A, Overgaag K, Vanmaekelbergh D and Vos W L 2004 *Nature* **430** 654
- [38] Anderson P W 1958 *Phys. Rev.* **109** 1492
- [39] Wiersma D S, Bartolini P, Lagendijk A and Righini R 1997 *Nature* **390** 671
- [40] Schwartz T, Bartal G, Fishman S and Segev M 2007 *Nature* **446** 52